



Manufacturing Engineering Society International Conference 2017, MESIC 2017, 28-30 June 2017, Vigo (Pontevedra), Spain

## Contact mechanics applied to the machining of thin rings

M. Estrems<sup>a\*</sup>, J. Carrero-Blanco<sup>a</sup>, W.E. Cumbicus<sup>b</sup>, O. de Francisco<sup>a</sup>, H.T. Sánchez<sup>a</sup>

<sup>a</sup> *Materials and Manufacturing Engineering Department, Univ. Politécnica de Cartagena, C/ Doctor Fleming s/n, Cartagena 30202, Spain*

<sup>b</sup> *School of Engineering, TECNUN, Univ. De Navarra, P° de Manuel Lardizabal, 13. Donostia-San Sebastián. Gipuzkoa 20018, Spain*

---

### Abstract

Precision machining of thin rings is of key importance in the performance of many mechanical components such as bearings, rings, turbines, etc. An important factor to take into account is to know the influence of the clamping forces values at different angular positions of the workpiece in the geometrical tolerances after machining. The lower the clamping force, better tolerances will be achieved, but with the disadvantage of reducing friction force and, therefore, increasing the risk of slipping. Therefore, achieving a minimum but safe clamping force is a key factor to control the process. This paper presents some contributions of contact mechanics to the determination of an optimum clamping force. A subsequent methodology is applied that takes into account model of bulk deformation and local contact stresses and experimental data with the object of obtain the optimum torque applied to the chuck.

© 2017 The Authors. Published by Elsevier B.V.

Peer-review under responsibility of the scientific committee of the Manufacturing Engineering Society International Conference 2017.

*Keywords:* Contact Mechanics; Turning; Thin Rings; Chucks; Friction coefficient.

---

### 1. Introduction

The design of lathe chucks to hold the thin ring workpieces takes into account the calculation of the minimum limit clamping force to be applied, thus provoking the minor possible effect on deformation, and therefore on the part precision loss [1], especially if these are slender as the case of thin rings [2, 3], which are common parts in gearboxes, motors, gear rims, pulleys, etc. These rings are required with a high degree of roundness and tight tolerances. The

---

\* Corresponding author. Tel.: +34 968 32 59 61

E-mail address: [manuel.estrems@upct.es](mailto:manuel.estrems@upct.es)

clamping forces of the jaws over a highly flexible ring cause a ring deformation that creates roundness errors in the part. The lower the clamping force, better tolerances will be achieved, but with the disadvantage of reducing friction force and, therefore, increasing the risk of slipping. However, if the clamping force decreases below a minimum limit, the detachment of the workpiece could occur, which what can lead to serious accidents [4]. Therefore, achieving a minimum but safe clamping force is a key factor to control the process.

Another factor to take into account is the spindle speed, as it increases, the clamping force decreases as a consequence of centrifugal forces, and the dynamic response of the system affects also the cutting process [5, 6]. Therefore, the clamping force must overcome factors such cutting forces, centrifugal forces, bending moments [7], vibrations [8], etc.

Usually, the rings are made in lathes that have concentric plate clutches and these are fixed mechanically by wrenches or hydraulically through the control of pressure by solenoid valves. In order to measure the clamping forces, there exist load cells, but these sensors are expensive and difficult to assembly. Due to the disposition of jaws, and the concentric mechanism, the three-jaw chuck is the most common kind of fixture for these components. There are some specialize fixtures for thin rings as the six-jaw chuck and the use of segmented jaws but they have some inconveniences as the hyperstaticity, the lack of flexibility, the expensiveness, etc.

In the literature, some formulations and methods are provided for calculations of stresses and deformation in rings placed on lathe chucks. The most common method is the use of the Finite Element Method (FEM) [9], but it has a high computational cost because it requires a fine mesh to achieve sufficient precision. One analytical method is developed by Malluck and Melkote [10] based on some formulae of an old book from which the expressions of the internal moment and the ring deformation are deduced. This method was checked experimentally and with the Finite Element Method (FEM).

Since the analytical method is quicker than that of the (FEM), many papers are based in this. For example, Kurnady et al. [11] used it in optimization of the machining operation. Sölter et al. [12, 13], used it in a model to predict errors using different fixturing strategies. Stöbener et al. [14] used it as an analytical tool to study different strategies such as ultrasonic sensing and the use of Fast Tool Servo for the compensation of errors in real time. Soleiman and Mehr [15] use this approach also, etc.

In order to avoid the above mentioned problems, in this paper the numerical and analytic calculation to obtain the contact stresses within the jaw-workpiece contact zone described in [16] is applied with some improvements such the calculation of the rigidity of jaws and the reaction in jaws to the cutting force, which is presented in this paper. A simple and economical integrating method is proposed, which reduces on the one hand, the 6 unknowns to 3 of the hyperstatic problem, taking into account the rigidity of the jaw-piece system, seen in [16]. Another the drawback of simplified calculation of Melkote [10] is due to suppose the reaction of the jaws in a point, which causes peaks of tension in the results that are not real, but through an area which depends on the geometry and elastic constants, so contact mechanics theory must be applied in order to get the real stresses in this zone as is done in this paper.

Moreover, in this paper the local stresses are evaluated through the contact mechanics applying Hertz for small contact, and the method developed by Carrero-Blanco [17] for large contact, where the contact width is in order of magnitude of the radius such as in segmented jaws. The use of contact mechanics theory, therefore, limits the value of the moment and allows superimposing the global tensions calculated by Castigliano's theorem [16] with the local tensions calculated by contact mechanics [17].

Another important factor of contact mechanics analyzed in this study is the calculation of adherent friction. The Coulomb's coefficient of friction cannot be assumed, because the materials and the state of the surfaces vary, so it is advisable to obtain experimental friction coefficient directly through a simple test in the same conditions of contact jaw-workpiece as in the turning operation. In this paper the method is presented and the friction coefficient of several materials have been calculated from data obtained from the instrumented ring presented in [18] and the use of several dynamometric wrenches. The clamping force on the jaws can vary with the tightening torque applied, so a method is proposed to obtain both, the multiplier factor  $k$  and the coefficient of friction  $\mu$ . The knowledge of  $\mu$ , will allow to obtain the Cattaneo's stick-slip zone pressures [19] and the subsequent map of subsurface stresses [20] that will superimpose the global stresses only when the contact area is small and large stresses.

## 2. Model of ring global stresses

In this section, a method for calculation of reaction in jaws is presented when a cutting force is applied to the ring clamped in the lathe. It presents some improvements to the procedure applied in [16]. In Fig. 1, the development of the model presented is shown, which uses the Castigliano’s Theorem for calculating the bending moments along the ring perimeter. The clamping forces  $P_i$  are introduced only if acting on the sector of the ring studied. The equilibrium conditions, the symmetry of the problem, the uniformity of the ring and the absence of friction, result in that all three  $P_i$ ’s are equal in magnitude to  $P$ .

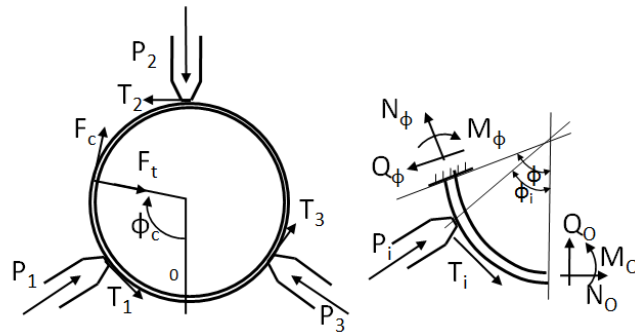


Fig. 1. Forces acting on the ring, and a sector of the ring.

From the sector of the ring, according to Fig. 1, the balance equations are [16]:

$$\begin{aligned}
 M(\phi) &= M_0 + rQ_0 \sin(\phi) + N_0 r(1 - \cos(\phi)) + P_i r \sin(\phi - \phi_i) + T_i r(1 - \cos(\phi - \phi_i)) \\
 Q(\phi) &= N_0 \sin(\phi) + Q_0 \cos(\phi) + P_i \cos(\phi - \phi_i) + T_i \sin(\phi - \phi_i) \\
 N(\phi) &= -Q_0 \sin(\phi) + N_0 \cos(\phi) - P_i \sin(\phi + \phi_i) + T_i \cos(\phi - \phi_i)
 \end{aligned}
 \tag{1}$$

The ring is assumed to be a rigid solid having three motions  $\delta_x$  and  $\delta_y$  and one rotation  $\delta_\theta$  in the center of the ring. The jaws have a normal and tangential stiffness  $k_n$  and  $k_t$ , which are the same for all three.

By introducing the cutting force, the reaction in the jaws presents 6 unknowns for 3 static equilibrium equations.

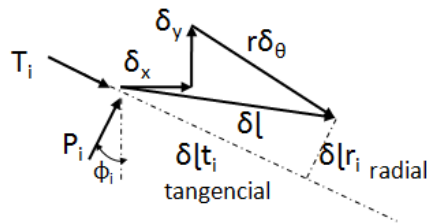


Fig. 2. Orthogonal decomposition of displacements.

From Fig. 2, the following relations between solid rigid displacements ( $\delta_x$ ,  $\delta_y$ ,  $\delta_\theta$ ) and local displacements ( $\delta_r$ ,  $\delta_t$ ) are obtained in each jaw ( $i$ ):

$$\begin{aligned}
 \vec{\delta} &= \vec{\delta}_x + \vec{\delta}_y + r\vec{\delta}\theta = \vec{\delta}_t + \vec{\delta}_r \\
 \delta_t &= r\delta\theta + \delta_x \cdot \cos \phi_i - \delta_y \cdot \sin \phi_i \\
 \delta_r &= \delta_x \cdot \sin \phi_i + \delta_y \cdot \cos \phi_i
 \end{aligned}
 \tag{2}$$

Supposing a rigidity of the jaw normal  $k_n$  and tangential  $k_t$ , the reactions of the jaw are:

$$\begin{aligned}
 P_i &= k_n \cdot \delta_{r_i} \\
 T_i &= k_t \cdot \delta_{t_i}
 \end{aligned}
 \tag{3}$$

Applying equilibrium of momentum and the balance of forces neglecting the difference of radius of the applied forces in external surface  $T_i$  and the cutting force  $F_c$ :

$$\sum T_i + F_c = 0 \quad (4)$$

$$0 = \sum (P_i \cdot \cos \phi_i - T_i \cdot \sin \phi_i) + F_c \cdot \cos \phi_c + F_t \cdot \sin \phi_c \quad (5)$$

$$0 = \sum (P_i \cdot \sin \phi_i + T_i \cdot \cos \phi_i) - F_t \cdot \cos \phi_c + F_c \cdot \sin \phi_c$$

Then, using the reference system of Fig. 1 in equation (2):

In point 1:

$$\delta l_r = \delta_y$$

$$\delta l_t = r \delta_\theta + \delta_x$$

In point 2:

$$\delta l_r = 0.5\sqrt{3}\delta_x - 0.5\delta_y \quad (6)$$

$$\delta l_t = r \delta_\theta - 0.5\delta_x - 0.5\sqrt{3}\delta_y$$

In point 3:

$$\delta l_r = -0.5\sqrt{3}\delta_x - 0.5\delta_y$$

$$\delta l_t = r \delta_\theta - 0.5\delta_x + 0.5\sqrt{3}\delta_y$$

Substituting (6) in (3),  $P_i$  and  $T_i$  can be obtained on all parts of the jaws:

$$k_n \cdot \frac{3}{2} \delta_x + k_t \cdot \delta_x (1 + 0.5) = F_c \cdot \cos \phi_c - F_t \cdot \sin \phi_c \quad (7)$$

$$k_n (\delta_y - 0.5\delta_y) + k_t (3 \cdot 0.5\delta_y) + F_t \cdot \cos \phi_c + F_c \cdot \sin \phi_c = 0$$

$$k_t (3r\delta_\theta) - F_c = 0$$

This is an equation system which solution is:

$$\delta_x = \frac{F_c \cdot \cos \phi_c - F_t \cdot \sin \phi_c}{1.5(k_n + k_t)} \quad (8)$$

$$\delta_y = \frac{-F_t \cdot \cos \phi_c - F_c \cdot \sin \phi_c}{1.5(k_n + k_t)}$$

$$\delta_\theta = \frac{F_t}{3rk_t}$$

Known  $P_i$  and  $T_i$ , substituting (8) in (3), the equilibrium is checked and we are in a position to apply equation (1) to obtain momentum, compression and cut diagram in all sections of the ring.

In order to get  $M_\theta$ ,  $Q_\theta$  and  $N_\theta$ , these are calculated through the three conditions given by the continuity in point 0 in Fig.1. i.e. for  $\phi=2\pi$ , then  $M_\phi=M_0$ ,  $Q_\phi=Q_0$ ,  $N_\phi=N_0$ , and  $\delta_r=0$ ,  $\delta_t=0$  and  $\delta_\theta=0$ . To calculate  $\delta_r$ ,  $\delta_t$  and  $\delta_\theta$ , the Castigliano's Theorem is used. To obtain the values at the singular points in the transitions, i.e. the reaction in the jaws, the contact mechanics has been taken into account in the jaw-ring contact system.

$M_\theta$ ,  $Q_\theta$  and  $N_\theta$ , are calculated in such a way that the continuity in  $\delta_r(\phi)$ ,  $\delta_t(\phi)$  and  $\delta_\theta(\phi)$  is given in point 0 when  $\theta=0$  and  $\theta=2\pi$ , in the way is showed in [16]. Once  $M_\theta$ ,  $Q_\theta$  and  $N_\theta$  are obtained, global stresses are obtained for the critical parts.

### 3. Contact mechanic in ring clamped in the chuck

From the study of the global tensions calculated by Castigliano’s Theorem, singular points are observed in the contact zones between the jaw and the ring (see Fig. 3), which offer tension peaks that are not real they are singular points that depends of the discretization of the problem. In fact, there is a distribution between each jaw and the ring on the contact surface as shown in Fig. 4. In order to establish the real values of the tensions produced in the jaw-ring contact zones, it is necessary to implement the local study of these stresses by the contact mechanics. These local stresses will overlap with the stresses obtained in the global study using the superposition principle. For small contacts, Hertz’s classic elastic contact model is used. For those in which the contact half-width is in the order of magnitude of the radius, such as in segmented jaws, the methodology developed by Carrero-Blanco in [17] will be applied (see Fig. 5).

#### 3.1 Hertz theorem. Small contact width

For situations in which the contact width cannot be considered in the order of magnitude of the ring radius, the classical equations of Hertz’s theory are applied:

$$a = \sqrt{\frac{4 \cdot R_{eq} \cdot \frac{P}{L}}{\pi \cdot E}} \tag{9}$$

$$P_{(Hertz)} = \frac{a \cdot E}{2 \cdot R_{eq} (1 - \nu^2)} \tag{10}$$

Where  $P$  is the normal force applied externally in each jaw,  $L$  is the length of the jaw,  $\nu$  is Poisson’s coefficient,  $E$  is the Young modulus, and  $R_{eq}$  is the equivalent radius of curvature in contact point, which is obtained as a combination of the radius of the tip of the jaw and the radius of the ring according to equation (11). If the contact is internal  $R_{ring}$  will be negative.

$$R_{eq} = \frac{1}{\frac{1}{R_{jaw}} + \frac{1}{R_{ring}}} \tag{11}$$

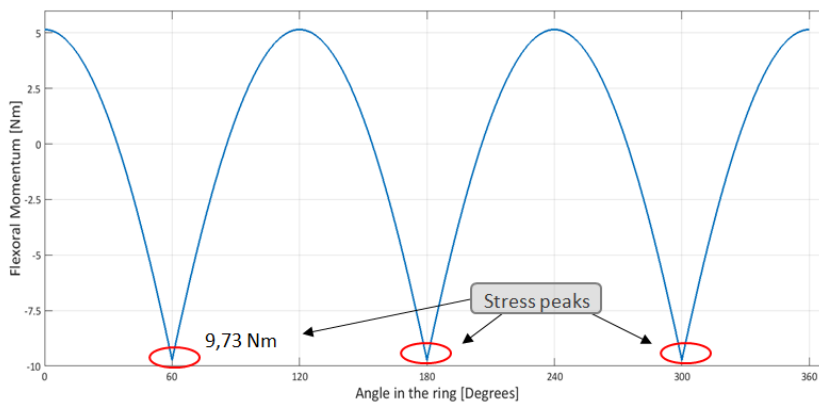


Fig. 3. Bending moment of the ring with a clamping force of 930 N without taking into account the contact mechanics.

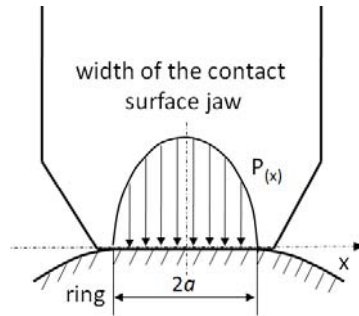


Fig. 4. Distribution of pressures in contact width of the jaw.

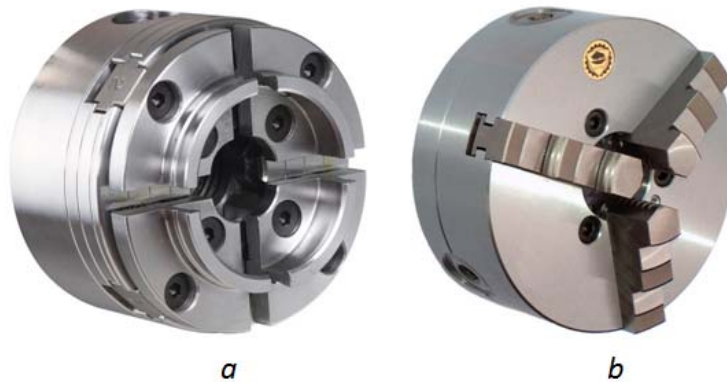


Fig. 5. a) Segment lathe chuck. Large contact. b) Normal lathe chuck. Small contact.

### 3.2 Large contact width

In cases where the contact width is of the order of magnitude of the radius, i.e. large contact widths such as when segmented jaws are used, the Hertz approximation is not valid, and the Carrero-Blanco [17] method is applied:

$$p(x) = \frac{E \cdot a \left( \frac{R_{\text{ring}}}{R_{\text{jaw}}} - 1 \right)}{2\pi(1-\nu^2)\sqrt{a^2-x^2}} \left[ \int_{-1}^1 \frac{\tan\left(\frac{a \cdot t}{R_{\text{ring}}}\right) \sqrt{1-t^2}}{\cos\left(\frac{a \cdot t}{R_{\text{ring}}}\right) \cdot \left(t - \frac{x}{a}\right)} \delta t - \int_{-1}^1 \frac{\tan\left(\frac{a \cdot t}{R_{\text{ring}}}\right) \sqrt{1-t^2}}{\cos\left(\frac{a \cdot t}{R_{\text{ring}}}\right) \cdot (t-1)} \delta t \right] \quad (12)$$

This expression is the pressure distribution in contact zone given a half-width of contact  $a$ . This integral is calculated through the quadrature norms of the Cauchy Principal Values, and the half-width  $a$  is determined by the secant method. Finally, a numerical method for the determination of a tensional map to the surfaces in contact of jaws and ring was developed by Estrems [20].

### 3.3 Influence of friction coefficient on the contact stress.

For those cases in which the contact area is small and the stresses are large, the knowledge of  $\mu$  allows to obtain the Cattaneo's stick-slip zone [19], and therefore, to determine the map of subsurface stresses [20] to overlap the global stresses. If Fig. 6, the normal pressure  $p(r)$  and the tangential pressure  $q(r)$  due to friction are represented in a cylindrical contact on the left, and a map of principal shear stress is represented on the right. As it is observed in the map, the value and depth of the critical point is very similar that given by the Hertz theory approximation in this case.

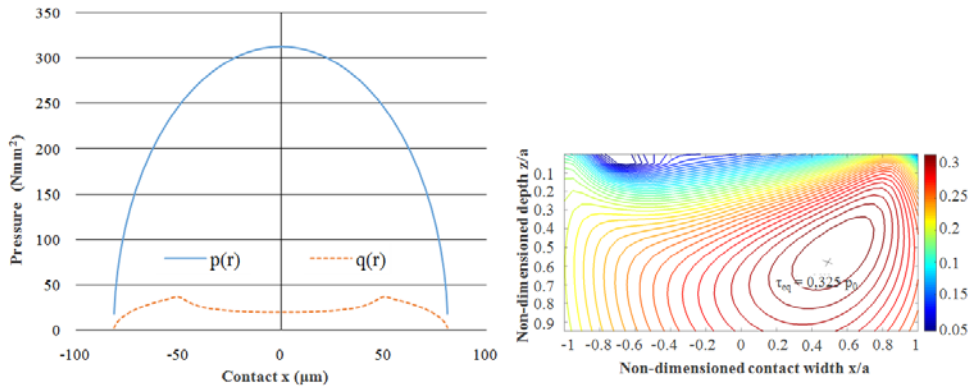


Fig. 6. Normal and tangential pressure distribution, and stress map in contact zone in a clamping with  $T=40\text{ N}$ ,  $P=400\text{ N}$ ,  $\mu=0,15$ . Aluminum ring 80 mm in diameter and 10 mm in width and planes jaws.

### 3.4 Experimental measurement of the coefficient of friction

In order to know the tightening force respect to the torque applied to the lathe chuck, a method comprising several steps has been experimentally tested. In [18], a simple method is described to obtain the normal force  $P$  applied to the ring by each jaw when a torque is applied to the chuck by a dynamometric wrench. This method uses an Aluminum ring instrumented with gages at certain symmetrical positions in order to know the deformation values in the ring. In this way, the multiplier factor of the mechanism of the chuck is obtained.

In addition to the normal force  $P$ , it is necessary to measure the torque at which a cylinder made of the material in study begin to slide in order to get the real friction coefficient  $\mu$  between the jaw and workpiece in real conditions. A simple method, which is described below, with accessible tools, has been developed and presented in this paper, so that it is possible to obtain reliable values of the tightening torque necessary for the ring does not slide during machining in such a way that its deformation due to clamping is minimal, thus improving the precision of the ring after the machining.

The method consists of measuring sliding friction values from different metals using a dynamometric wrench BACHO 7455-60 with has a calibration certificate.

In the process a fixed torque is applied by the dynamometric wrench on the chuck which corresponds to a normal force  $P$  applied to the jaw, and an incremental torque is applied to the screw centered on the piece, as shown in Fig. 7 until the sliding begins.

The steps to obtain the coefficient of friction are as follows:

- Place the metallic piece (showed in Fig. 7) in the chuck lathe.
- Tighten the screw chuck lathe with the dynamometric wrench. Starting at  $2\text{ N}\cdot\text{m}$  and climbing successively.
- Tighten the workpiece screw with a torque controlled by the dynamometric wrench until the workpiece slides.
- Repeat the process for different clamping forces, so that a determined value of friction is obtained.

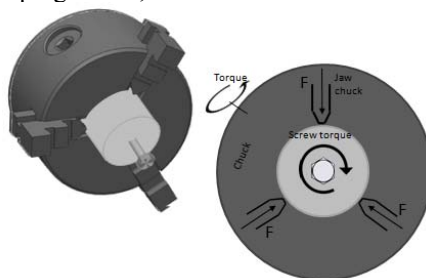


Fig. 7. Example of piece fixed in the jaw chuck. Forces and moments applied to measure friction.

#### 4. Conclusions

A study of contact mechanics during the fixture of thin rings to lathes has been performed. An improved formulation to obtain the reaction in jaws to the cutting forces has been developed, but the main body of the paper have been focused in the application of the contact mechanics theory and in the experimental determination of the friction coefficient.

The friction coefficient is an important factor to determine the clamping force of the ring in a safety way. So in this paper a procedure has been presented to get the friction coefficient in the same place, the same components and in the same conditions as they are going to work.

Moreover, a study of the local stresses due to the contact have allowed to refine the calculation of the torque given by the theory of Strength of Materials, and superimpose the local stress to global stresses taking into account the friction force. In this way, a local damage in the contact zone could be prevented.

#### Acknowledgements

The authors would like to thank the Basque Government for supporting this work made under the ETORTEK Program within the MARGUNE CRC framework while the first author was a visiting professor at TECNUN.

#### References

- [1] H.T. Sánchez, M. Estrems, F. Faura, *Int. J. Adv. Manuf. Technol.* 29 (2006) 426-435.
- [2] J. Sölter, C. Grote, E. Brinksmeier, *Proc. 12th CIRP Conference on Modelling of Machining Operations*. San Sebastián (SPAIN), Vol. 2, 2009, pp. 703-709.
- [3] L. Nowag, J. Sölter, E. Brinksmeier, *Prod. Eng.* 1 (2007) 135-139.
- [4] A. H. Slocum. *Precision Machine Design*, Prentice-Hall, Society of Manufacturing Engineers Dearborn (MI), USA, 1992.
- [5] M. Rahman, M. Tsutsumi, *J. Mater. Process. Technol.* 38 (1993) 407-415.
- [6] P. F. Feng, D. W. Yu, Z. J. Wu, E. Uhlmann, *Int. J. Mach. Tools Manuf.* 48 (2008) 1268-1275.
- [7] P. F. Feng, Z. J. Wu, D. W. Yu, E. Uhlmann, *J. Mater. Process. Technol.* 204 (2008) 124-129.
- [8] M. Rahman, Y. Ito, *J. Sound Vib.* 102 (1985) 515-525.
- [9] U. Heisel, C. Kang, *Prod. Eng.* 5 (2011) 151-158.
- [10] J. Malluck, S. N. Melkote, *J. Manuf. Sci. Eng.* 126 (2004) 141-147.
- [11] M. S. Kurnadi, J. Morehouse, S. N. Melkote, *Int. J. Adv. Manuf. Technol.* 32 (2007) 656–665.
- [12] J. Sölter, *Materialwissenschaft und Werkstofftechnik*, 40 (5□6) (2009), 380-384.
- [13] L. Nowag, J. Sölter, E. Brinksmeier, *Prod. Eng.* 1 (2007) 135-139.
- [14] J. Sölter, C. Grote, E. Brinksmeier, *Mach. Sci. Technol.* 15 (2011) 338-355.
- [15] D. Stöbener, B. Beekhuis *CIRP Ann. – Manuf. Technol.* 62 (2013) 511-514.
- [16] M. Estrems, M. Arizmendi, A. J. Zabaleta, A. Gil, Numerical Method to Calculate the Deformation of Thin Rings during Turning Operation and its Influence on the Roundness Tolerance. *Proceedings of 6th Manufacturing Society International Conference (MESIC 2015)*. Barcelona, Spain, 2015.
- [17] J. Carrero-Blanco, M. Estrems, H.T. Sánchez, *Rev. Int. Métodos Numéricos para Cálculo y Diseño en Ing.* 32 (2016) 240–251.
- [18] M. Estrems, M. Arizmendi, W. E. Cumbicus, A. López, Measurement of clamping forces in a 3 jaw chuck through an instrumented Aluminium ring. *Proceedings of 6th Manufacturing Society International Conference (MESIC 2015)*. Barcelona, Spain, 2015.
- [19] C. Cattaneo, *Rendiconti dell'Accademia Nazionale dei Lincei*. 27 (6) (1938) 342-348.
- [20] M. Estrems, F. Faura, J.I. Pedrero, *Rev. Int. Métodos Numéricos para Cálculo y Diseño en Ing.* 16 (2000) 455-470.